New Phytologist

Research

Rapid report

Visual quantification of embolism reveals leaf vulnerability to hydraulic failure

Author for correspondence:
Timothy J. Brodribb
Tel: +61 362261707
Email: timothyb@utas.edu.au

Received: *22 October 2015*
Accepted: *8 December 2015*

Timothy J. Brodribb[1], Robert P. Skelton[1], Scott A. M. McAdam[1], Diane Bienaimé[2], Christopher J. Lucani[1] and Philippe Marmottant[2]

[1]School of Biological Sciences, University of Tasmania, Hobart, Tas. 7001, Australia; [2]LIPhy UMR 5588, CNRS/Université Grenoble-Alpes, Grenoble F-38401, France

New Phytologist (2016)
doi: 10.1111/nph.13846

Key words: cavitation, drought, leaf hydraulic, optical, stomata, water stress, xylem.

Summary

- Vascular plant mortality during drought has been strongly linked to a failure of the internal water transport system caused by the rapid invasion of air and subsequent blockage of xylem conduits. Quantification of this critical process is greatly complicated by the existence of high water tension in xylem cells making them prone to embolism during experimental manipulation.
- Here we describe a simple new optical method that can be used to record spatial and temporal patterns of embolism formation in the veins of water-stressed leaves for the first time.
- Applying this technique in four diverse angiosperm species we found very strong agreement between the dynamics of embolism formation during desiccation and decline of leaf hydraulic conductance.
- These data connect the failure of the leaf water transport network under drought stress to embolism formation in the leaf xylem, and suggest embolism occurs after stomatal closure under extreme water stress.

Introduction

The risk of explosive invasion of air into the vascular system of plants during acute water stress places a limit on species' ability to survive during soil drought (Brodribb & Hill, 1999; Choat *et al.*, 2012). The abrupt formation of air-embolisms typically occurs during drought, when increasing tension in the water transporting xylem tissues exceeds a limit (termed the 'air-seeding' threshold) causing air to be pulled into the tubular hydraulic conduits (Tyree & Sperry, 1989). The resultant embolisms block xylem water transport, isolating leaves from their water source in the soil (Sperry & Pockman, 1993). Of particular interest is the fact that the air-seeding threshold is a largely conservative property of plant species (Choat *et al.*, 2012), thus providing a promising functional predictor of lethal water stress among different plant species (Brodribb & Cochard, 2009).

The study of vulnerability to damage in the plant water transport system, known as 'plant hydraulics', originates from the visionary work of early researchers who quantified the impact of air bubbles in the xylem on water transport (hydraulic conductance) of twigs (Tyree & Sperry, 1989). Since this time, the development of new techniques to measure the air-seeding threshold of stems has led to a degree of controversy surrounding the frequency of air-seeding and the ability of plants to repair embolisms (Rockwell *et al.*, 2014b). Opinions coalesce into two different schools; those who consider that embolism and embolism repair are routine in many woody species (e.g. Brodersen & McElrone, 2013; McCulloh & Meinzer, 2015), and those who find that embolisms are a symptom of acute water stress and that they can only (occasionally) be repaired under moist conditions in the presence of positive pressure from roots (Cochard & Delzon, 2013). A corollary of the routine-embolism-and-repair theory is that two adaptive axes exist for plants growing under water stress; either to resist air seeding; or to more efficiently repair embolism. Alternatively, the rare-embolism theory views resistance to embolism as the only adaptive pathway that can enable the maintenance of xylem function during significant soil drying. These are two very different scenarios, with very different implications for plant evolution. Hence there is an urgent need to resolve this schism, because the physiology of plant water transport lies at the heart of a great many aspects of plant ecology and evolution, and its progress is being hindered by a lingering debate between proponents of these different schools.

Technical uncertainty is largely responsible for the persistence of contrasting perspectives on vulnerability to embolism, and in particular, uncertainly about the behaviour of embolisms in stems that must be cut from the tree before they can be measured (Wheeler *et al.*, 2013). For this reason there has been substantial interest in noninvasive techniques that can detect embolisms nonintrusively. The detection of acoustic emissions produced by cavitation is being employed with increasing confidence (Ponomarenko *et al.*, 2014; Nolf *et al.*, 2015), while tomographic methods using X-rays can provide detailed evidence of when and where embolism occurs in woody stems (Brodersen *et al.*, 2013; Choat *et al.*, 2015). Here we present results from a new optical method that provides the best evidence yet of the timing and spread of embolisms in the leaf venation system during water stress. Our technique develops upon early work showing that embolized vessels in stems can be recognized by their relatively high reflectance compared with water-filled conduits (Haines, 1935). Rather than relying on dyes to quantify the effects of embolism on water flow (Salleo *et al.*, 2001; Triflio *et al.*, 2003), we use new image processing that detects dynamic embolism by recording rapid changes in the transmission of light through the veins of leaf samples, thus enabling embolisms to be filmed and mapped during the development of leaf water stress.

Leaf hydraulic performance is a sensitive indicator of plant photosynthetic performance, ecology and evolution (Sack & Scoffoni, 2013). Furthermore, the vulnerability of leaves to hydraulic dysfunction during water stress has proved highly informative about the timing of plant death, and the mechanisms of adaptation to increasing aridity (Blackman *et al.*, 2010; Brodribb *et al.*, 2014). However, leaf hydraulic techniques to date have proven more laborious than equivalent measures in stems. By overcoming this technical hurdle, the new optical vulnerability (OV) technique described here holds great promise as a cheap and easy method for assessing leaf vulnerability in a wide variety of plant species. We compare the timing of embolism as determined by the novel OV method with classic hydraulic techniques to determine whether the timing of optical observations of embolism spread in leaves corresponds with measured losses in leaf hydraulic conductance or leaf cell turgor.

Materials and Methods

Plant material

Four angiosperm species from different families were chosen to compare the traditional hydraulic vulnerability techniques with the OV method. *Eucalyptus globulus* Labill. (Myrtaceae) is a large tree used commonly in silviculture worldwide, *Bursaria spinosa* Cav. (Pittosporaceae) is a central and eastern Australian desert/dry forest shrub, *Eucryphia moorei* F.Muell. (Cunoniaceae) is a tree species restricted to rainforest in eastern Australia, and *Senecio minimus* Poir. (Asteraceae) is a common ruderal herbaceous species found in temperate forests of Australia and New Zealand, from a genus with a global distribution. These species were chosen because they grow under very different native rainfall climates and were thus expected to display a range of xylem vulnerabilities. In the case of woody species, all material was harvested from single representative trees growing in the grounds of the University of Tasmania. Whole plants of the herbaceous species were harvested from a small population of plants growing in drainage channels near the University of Tasmania glasshouse facility. All material was sampled during the wetter winter months of June to August 2015.

For both vulnerability techniques, large branches (2–3 m) of woody species or whole rooted individuals of the herb were sampled early in the morning. The large branch size was sampled to ensure that no vessels were continuous between the site of stem excision and the leaf venation. This was tested by pressurizing the cut end of branches with air at 1 Bar, and excising petioles of leaves downstream underwater until bubbles were seen to emerge from the petiole, indicating open vessels.

Optical vulnerability

Each tree was represented by three branches, brought directly into the laboratory upon excision, where a single leaf was placed under a stereomicroscope (M205A; Leica Microsystems, Heerbrugg, Switzerland) while remaining attached to the large parent stem. Leaves were carefully fixed to the microscope stage using transparent adhesive tape, ensuring that the stomatal surface was not occluded. The target leaf was illuminated homogeneously from below at an intensity of *c.* 40–80 μmol quanta to produce a transmitted light image which was captured on a digital camera (DFC450; Leica Microsystems) attached to the microscope. Leaves with bundle sheath extensions produce the clearest images, but homobaric leaves are also suitable, although minor veins are often difficult to resolve. Magnification was set to provide sufficient resolution of the larger vein orders on the leaf (×8–10, providing between 2400 and 3600 pixels per inch resolution), and photographs were taken every 30–60 s until a browning of the leaf was observed (typically indicating the death and lysis of mesophyll cells). Higher magnification can provide better resolution of individual conduits but this comes at a cost of a smaller field of view. Here we opted for a larger (8.2 mm) field of view to enable good visualization of multiple vein orders. Desiccation ranged in time from 1 to 4 d during which time the water potential of adjacent leaves (ψ_{leaf}) was sampled using a Scholander pressure chamber (PMS, Albany, NY, USA) *c.* every 1–3 h (with sampling gaps overnight between 19:00 h and 07:30 h). At each time point 2–3 leaves were sampled to ensure homogeneity in ψ_{leaf}. In species with larger leaves a psychrometer (ICT International, Armidale, NSW, Australia) was attached to an adjacent leaf to provide a continuous measure of water potential during drying. These adjacent leaves were maintained at 22°C under laboratory lighting, and at a temperature within 1°C of the target leaf. In all species we found that after stomatal closure, the rate of decline of ψ_{leaf} was highly linear, enabling a very confident prediction of ψ_{leaf} of the target leaf at any time. Linear regressions between leaf water potential and time since excision for each sampled branch were used to describe the change in ψ_{leaf} as branches dehydrated.

Analysis of the image sequence captured during desiccation was carried out to identify rapid changes in light transmission through leaf veins that corresponded to air entry into the xylem conduits

(Ponomarenko *et al.*, 2014). This was done using an image subtraction method in ImageJ to highlight changes between successive images in the stack of images produced during the branch drying process. The image subtraction method highlights rapid changes in light transmission caused by bubble expansion, while filtering all other slow movement associated with drying. An advantage of the image subtraction method is that multiple events could be observed in any pixel, thus allowing resolution of multiple embolisms occurring in xylem cells that may overlay each other. A new image stack comprised of subtracted images was then thresholded to highlight the embolism events, which appeared as white pixels on a dark background. After thresholding, the 'analyse particles' function of ImageJ (National Institute of Health, New York, NY, USA) was used to filter out noise, which appeared as small random changes in pixel contrast compared with the large, structured embolism events. A cumulative 'Z-projection' of all the thresholded image sequence produced a map of the sum of all embolisms, and this was then used to separate veins into three orders: midrib, 2° (large veins emerging from the midrib and traversing more than half the distance to the margin before bifurcating) and 3° (all remaining veins). A similar function 'Timelapse Colour Coder' was used in some cases to produce colour maps of the timing of embolism throughout the vein network. Regions of interest corresponding to each vein order were then created and the 'Measure Stack' function used to measure the number of cavitated pixels in each image for each vein order throughout the image stack. This function measures the number of pixels above the threshold (defined by being embolized – black or non-embolized – white) in each slice of the image stack. The count of embolized pixels was then summed to give the cumulative number of pixels present in each vein order over time. The product is a temporally and spatially resolved data set indicating the accumulation of embolisms in vein orders. The abrupt start and finish of embolization during leaf drying enabled the dynamic spread of embolism to be expressed as the percentage of a maximum embolized state in each vein order at each time point (corresponding to the acquisition time of each new image). By converting time into ψ_{leaf} for each movie, an optical vulnerability curve was produced for the different vein orders of each leaf.

Hydraulic vulnerability

Three large branches were taken from the same trees as used for OV measurements, except in the case of *S. minimus* where three whole plants with roots were harvested from the same small population of individuals growing on loose gravel. All plants were sampled in the morning during the wetter months of May to August such that branches were initially hydrated at near −0.5 MPa. Samples were bagged and transported to the laboratory where they were exposed to cycles of dehydration followed by equilibration in a humidified bag for at least an hour before measuring. Measurements were scheduled *c.* every 0.5 MPa until ψ_{leaf} could no longer be reliably measured. Dehydration was carried out at 20 ± 3°C and under a combination of laboratory and natural lighting of *c.* 50–100 μmol quanta m^{-2} s^{-1}. Leaf hydraulic conductance (K_{leaf}) was determined by measuring dynamic flow during leaf rehydration (Brodribb & Cochard, 2009). Briefly, leaves (or in the case of the microphyllous species *B. spinosa*, small shoots with 5–10 leaves) were cut underwater and immediately attached to a flowmeter (see http://prometheuswiki.publish.csiro.au/ for detailed instructions) while the hydraulic flux into the leaf was logged. After 30 s the leaf was removed and ψ_{leaf} determined after a 10 min equilibration period. Calculation of K_{leaf} was made using the equation; $K_{leaf} = F/\Delta\psi$, where F is the hydraulic flux into the leaf (in mmol m^{-2} s^{-1}); $\Delta\psi$ is the hydraulic driving force (equal to ψ_{leaf}). Two values of K_{leaf} were measured for each leaf, an initial value associated with the equilibrated ψ_{leaf} before leaf excision, and a final value after disconnection from the flowmeter. The two values were compared to ensure agreement within 30% variation. Values were discarded if variation exceeded 30% (*c.* 1% of cases). Values of K_{leaf} (initial) were plotted against initial ψ_{leaf} (before leaf excision) and a sigmoidal regression ($K_{leaf} = a/(1 + e^{(-(x-x0)/b)})$) fitted to data for each branch. From these regressions, using data from between 15 and 30 leaves per branch, three values of ψ_{50} (the water potential when K_{leaf} was reduced to 50% of the initial maximum − a) were calculated for each species.

Turgor loss point

To determine the point of stomatal closure we measured the water potential corresponding to bulk leaf turgor loss ψ_{tlp}. The point of bulk leaf cell turgor loss was determined in each individual by the relationship between ψ_{leaf} and water volume in the leaf. Branches from the same individuals as used for vulnerability assessment (or from neighbouring plants in the case of the herb *S. minimus*) were cut underwater and allowed to hydrate to > −0.1 MPa. From these branches at least three leaves per species were removed and measured using the bench drying technique (Tyree & Hammel, 1972). Leaf weight and ψ_{leaf} were measured periodically during slow desiccation of sample leaves in the laboratory. Desiccation of leaves continued until leaf water potentials stopped falling, or began to rise due to cell damage. Relative water content was plotted against ψ_{leaf} for each leaf, and the ψ_{leaf} at turgor loss point was determined as the point of inflection between the linear and nonlinear portions of the plot. A mean ψ_{leaf} at turgor loss ± standard deviation (SD) ($n = 3$) was calculated for each individual (or from three individuals in the case of *S. minimus*).

Results

Visualization of embolization

Leaves dried for long periods of time before the initial embolism events were observed as discrete events propagating within the venation between image frames. Incipient embolism was recorded between 4.75 h (in *S. minimus*) and 29 h (in *B. spinosa*) following the excision of branches or the removal of whole plants from the soil. Before this time the only differences between sequential leaf images were caused by motion produced due to slow tissue shrinkage as leaves desiccated. Initial embolisms were typically observed as very rapid (faster than the image sampling period of 30 s) invasion of air into larger veins and patches of closely

connected downstream minor veins (Fig. 1). The spread of embolism was rather patchy both temporally and spatially in all species, but the typical pattern observed was that embolisms in major veins were typically large events that passed between vein orders, while smaller 3° veins embolized in small steps that were randomly distributed across the leaf (Fig. 2). Embolism continued for periods ranging between 6.5 h (in *S. minimus*) and 32 h (in *E. globulus*) after which embolism ceased (Fig. 2) and leaves were usually observed to change colour, presumably associated with tissue death.

The progression of total cumulative embolism in the xylem network of each species approximately followed a logistic function when plotted against ψ_{leaf} (Fig. 3), although steps were always evident due to larger embolism events, particularly early in the embolism cycle. Although curves were similar for different leaves of the same species, there was enormous variation between species in the ψ_{leaf} range causing embolism. The form of these optical vulnerability relationships in the three representative leaves per species appeared to be very similar to the shape of hydraulic vulnerability curves from the same individuals (Fig. 3). A plateau in K_{leaf} during the first hours of leaf desiccation indicated a range of ψ_{leaf} which had no effect on the hydraulic conductance. This initial period of uncompromised water transport function was corroborated by a lack of embolism measured optically during the same, species-specific, range of ψ_{leaf}. The plateau in K_{leaf} was short in the vulnerable species *S. minimus* (< 12% decline of K_{leaf} until −1.67 MPa), but very long in hardy species such as *E. globulus* and *B. spinosa* where K_{leaf} was not observed to decline by > 12% until after −4.55 MPa, or > 3 d drying (Fig. 3).

Water potentials observed to produce 12%, 50% and 88% embolism or hydraulic dysfunction were very similar for both measures of vulnerability (Fig. 3). There was close to 1 : 1

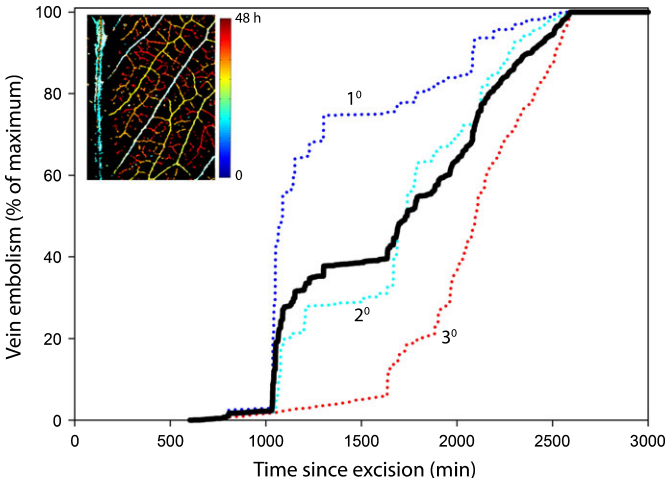

Fig. 2 The accumulation of embolisms over time is shown in different vein orders (dotted lines) of a desiccating *Eucalyptus globulus* leaf. Total embolism (the sum of all recorded embolisms – black line) shows that embolism begins *c.* 600 min after branch excision and continues for *c.* 2000 min. The spatial distribution of embolism (insert map) shows large events occurring early in the midrib and the latest events in the minor veins.

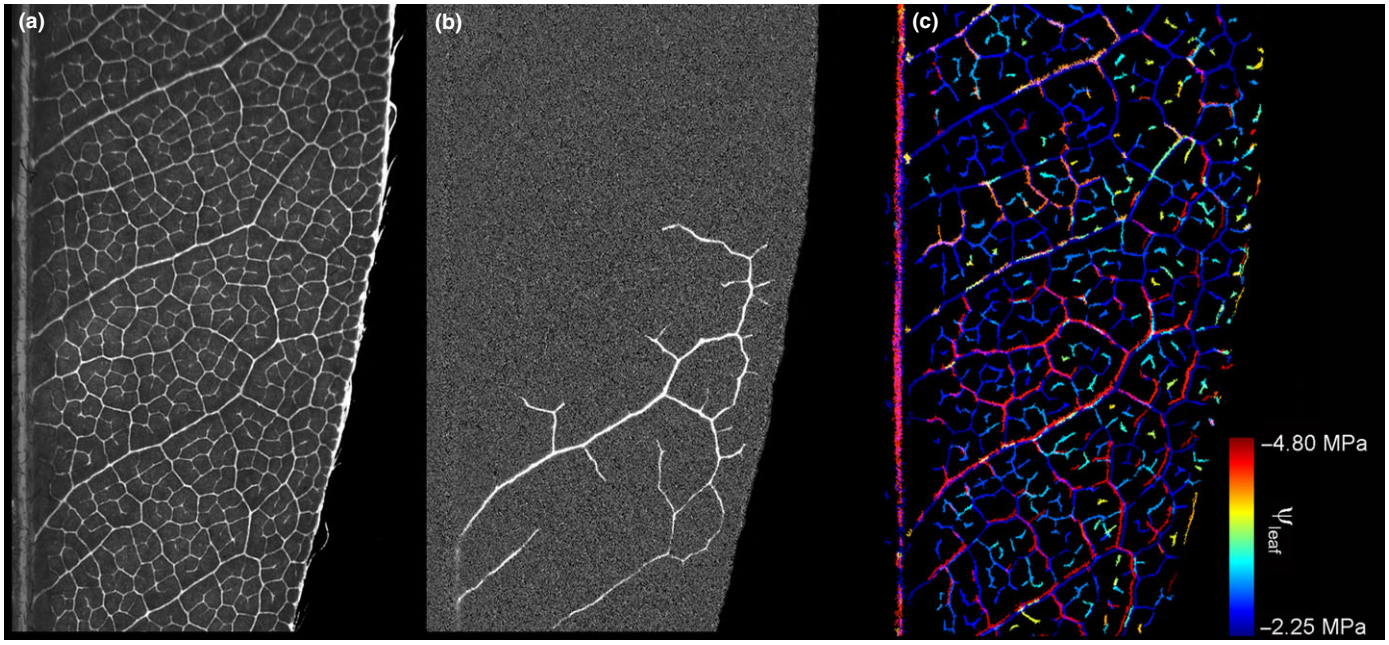

Fig. 1 (a) Image 1 from the series of images taken during the dehydration of a *Eucryphia moorei* leaf (half of the original image is shown). The transmitted light images highlight the majority of the vein network. (b) A single embolism event recorded by subtraction of sequential images 450 and 451 in the image stack (450 min after the branch was removed from the tree). Embolism causes an abrupt change in light transmission that appears as a vivid light area in the subtraction image. This event shows the propagation of a single embolism, presumably from the midrib, into the secondary and tertiary venation. (c) A colour map of all embolisms recorded during the desiccation of the same leaf over 2450 min shows the occurrence of embolisms in most visible veins. Larger veins are seen to experience multiple embolisms, seen as an overlay (addition) of different colours (colour legend shows the colour label assigned according to leaf water potential; no embolisms were observed until a leaf water potential of −2.24 MPa was reached).

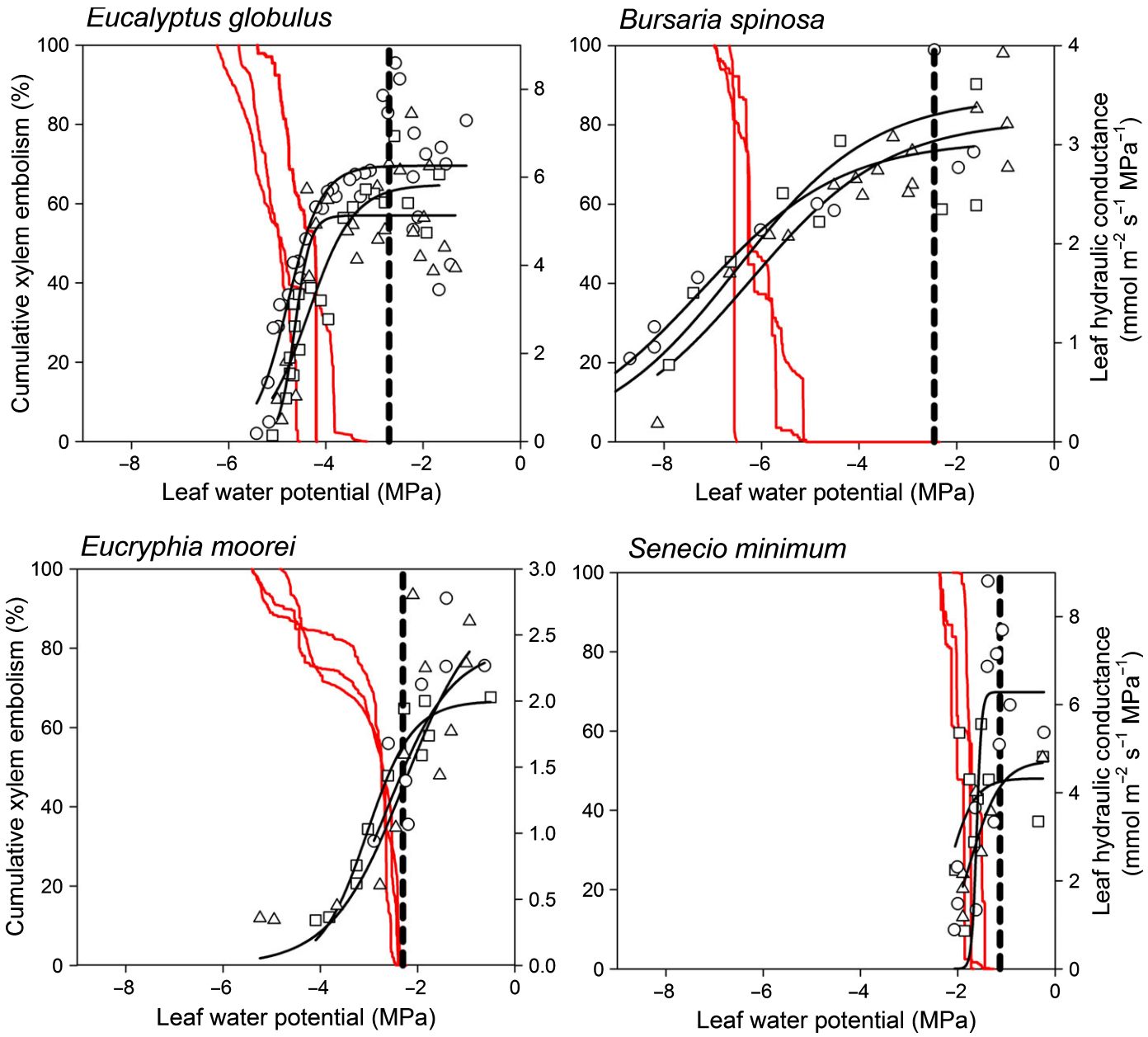

Fig. 3 Hydraulic vs optical vulnerability curves for the four species. Optical curves (red lines) show the percentage cumulative total embolism recorded during drying in three leaves from three different branches, while hydraulic curves (black) show the decline of K_{leaf} during drying in three branches. The dashed vertical line shows the mean turgor loss point for each species.

relationship between ψ_{leaf} observed to cause 50% embolism and 50% reduction in K_{leaf} over a very large range of vulnerabilities (mean ψ_{leaf} at 50% K_{leaf} ranged from -1.9 ± 0.28 MPa in *S. minimus* to -6.9 ± 0.41 MPa in *B. spinosa*). When comparing the ψ_{leaf} at 12% and 88% loss of function between techniques, most species showed similar trends, except the small leaved species *B. spinosa* (Fig. 4) which showed longer tails in the hydraulic compared with optical method.

The ψ_{leaf} at 50% loss of function was always found to occur after the turgor of leaf cells had fallen to zero. The mean point of incipient embolism (ψ_{leaf} at 12% embolism) also occurred after the mean turgor loss point in all species, but in the herbaceous species *S. minimus* and the rainforest tree *E. moorei* there was a very small margin between these two thresholds (Fig. 3; Supporting Information Fig. S1).

Discussion

We present a new optical method that allows the process of dynamic leaf embolism during water stress to be visualized for the first time. Employing this technique in four angiosperm species with contrasting water stress tolerances provided clear insight into fundamental questions regarding the impact of embolism upon water transport in leaves. Two important conclusions flow from our

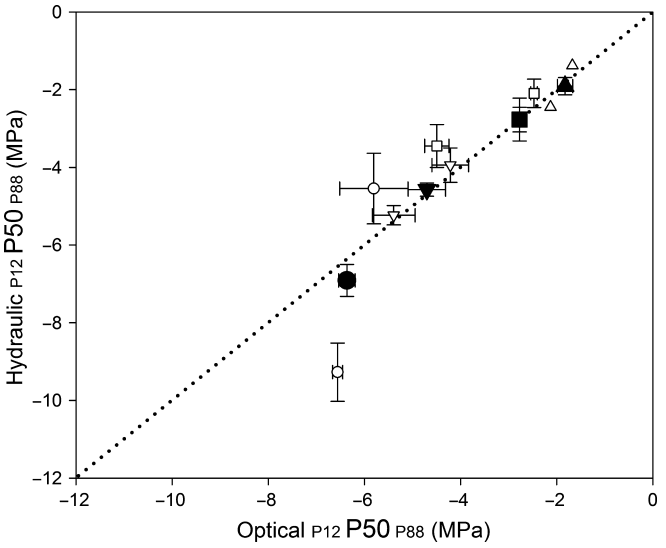

Fig. 4 Comparisons of water potentials at 12%, 50% and 88% loss of xylem function (P12, P50 and P88) in *Senecio minimus* (triangles), *Eucryphia moorei* (squares), *Eucalyptus globulus* (inverted triangles) and *Bursaria spinosa* (circles). For each species the mean P50s (closed symbols; error bars, standard deviation, $n = 3$) for both hydraulic and optical techniques agree very closely with the 1 : 1 line (dotted). Divergence of P12 and P88 (open symbols) in *Bursaria* indicates a steeper slope in the optical vs hydraulic vulnerability curves.

observations of water stressed leaves. First, we find that the water potential thresholds causing declining hydraulic conductance in leaves correspond very strongly with measured ψ_{leaf} thresholds for the spread of embolism in the leaf venation as determined by OV. Second, we observe that the point of incipient embolism in the leaf vein network occurs after the bulk leaf turgor loss, supporting other studies (Brodribb & Holbrook, 2003; Nardini *et al.*, 2003) indicating that stomatal closure generally pre-empts xylem embolism in the leaf.

Optical method

The OV method gives unprecedented resolution of the dynamics of embolism invasion into leaves. After many hours of drying, discrete embolisms could be easily observed rapidly propagating into the venation network. Although these embolisms could not be resolved to the level of individual conduits due to a technical trade-off between resolution and field of view, higher power magnification in wood samples has verified that source of the optical signal is due to a phase change from liquid to void in xylem lumina (Ponomarenko *et al.*, 2014). A very strong correlation between the dynamics of xylem embolism recorded by the OV method, and the decline of the hydraulic conductance of whole leaves, provides a compelling linkage of cause and effect.

In determining thresholds for embolism from optical data, no weighting was assigned to vein orders, thus every embolism was treated equally regardless of its position in the leaf vein network. This was despite the fact that larger vein orders appear more vulnerable than smaller veins (T. J. Brodribb *et al.*, unpublished) (Fig. 2). Additionally in some species there were minor vein orders that were not completely resolved in the microscope images. Although embolism in large veins close to the source of water supply to the leaf venation network (the midrib and petiole) should have a disproportionate influence on leaf water transport compared with distal venation, in the species examined here there was no evidence of biased effects of embolism in different vein orders. A likely reason for this is that low order veins (midrib and secondary venation) were highly composite in terms of conduit numbers, and were observed to embolize multiple times throughout the embolism cycle of minor veins (each of which only tended to embolize once; Fig. 1c). Thus it is likely that these larger veins retained some conductivity as leaves dried, only approaching zero conductivity once all other veins were air filled. This observation fits well with the redundancy arguments used to explain why leaf xylem networks in angiosperms are always characterized by a loopy, reticulate topology (Katifori *et al.*, 2010). The hierarchical, reticulate networks found in all species examined here thus provide an efficient means of bypassing local embolisms in the leaf water transport network, allowing the restoration of water delivery to the whole leaf, albeit with reduced efficiency, when a partially cavitated leaf is rewatered (Blackman *et al.*, 2010).

Declining K_{leaf} in water stressed leaves was generally observed once leaves crossed the threshold ψ_{leaf} at which incipient vein embolism was recorded by the optical method. Only in the toughest species, *Bursaria* was there a suggestion that K_{leaf} declined before embolism, but in this species it was necessary to use small shoots with many (> 20) tiny leaves to measure K_{leaf}, and it is likely that variation in embolism vulnerability of some of these leaves was different from the three representatives measured by the OV method. In all species, the point of incipient embolism was breached after leaves had lost turgor. Given that stomata generally close at or before turgor loss (Brodribb & Holbrook, 2003), this strongly suggests that stomata were closed in all species before embolism had begun (Fig. 2). Such a result is somewhat surprising in the light of recent studies that suggest declines in K_{leaf} may occur during or even before stomatal closure (Brodribb & Holbrook, 2004; Scoffoni *et al.*, 2014). The explanation for this discrepancy may emerge from the different methodologies used to determine leaf vulnerability. The hydraulic technique employed here measures K_{leaf} in samples that have been highly equilibrated (nonevaporating for > 3 h), such that ψ_{leaf} measured by the pressure chamber represents a homogeneous pressure across the entire leaf. Under these circumstances, the gradient driving water uptake in the leaf is well known, and K_{leaf} gives a value of conductance between the petiole and the mesophyll. By contrast, methods that assess K_{leaf} in samples that are evaporating, suffer the uncertainty that the pressure gradient across the leaf is a function of the evaporation rate, and cannot be measured. In addition, evaporation within the leaf can provide a nonhydraulic pathway for transfer of water between tissues, potentially increasing the apparent K_{leaf} (Rockwell *et al.*, 2014a; Buckley, 2015). Thus the evaporative method of K_{leaf} determination provides an estimate of how transpiration affects K_{leaf}, but probably does not give a clear indication of how embolism affects K_{leaf}. The clear result from data presented here is that K_{leaf} declines under severe water stress due to the invasion of embolisms into the leaf venation.

Implications for embolism theory

These results indicate that for the ecologically diverse woody plant species sampled here, xylem embolism by desiccation only occurs once leaves are sufficiently water-stressed to completely close stomata. Given the proximity of turgor loss and incipient embolism in *S. minimus*, a possibility remains that, under exceedingly high vapour pressure gradients, stomatal closure and embolism may overlap in this herbaceous species. However it seems unlikely that the rate of desiccation in the excised branches used here will ever be exceeded by plants in the field. Thus our data support the theory that embolism in the leaf xylem is a rare event in nature, associated with acute and damaging water stress. The OV method we present here is compelling in its ability to vividly resolve embolism in action. The technique provides powerful insight yet its simplicity should allow its broad application to a diversity of physiological and ecological questions associated with xylem embolism in plants.

Acknowledgements

The authors gratefully acknowledge funding support from the Australian Research Council DP140100666 (T.J.B.), DE140100946 (S.A.M.M.), the University of Tasmania for visiting scholar exchange funding (P.M.), and European Research Council under the European Community's Seventh Framework Programme (FP7/2007-2013) ERC Grant Agreement Bubbleboost no. 614655.

Author contributions

T.J.B. and P.M. designed the method. T.J.B. planned and designed the research. T.J.B., R.P.S., S.A.M.M., C.J.L. performed experiments, T.J.B., R.P.S., D.B. analysed data, T.J.B. wrote the manuscript.

References

Blackman CJ, Brodribb TJ, Jordan GJ. 2010. Leaf hydraulic vulnerability is related to conduit dimensions and drought resistance across a diverse range of woody angiosperms. *New Phytologist* **188**: 1113–1123.

Brodersen CR, McElrone AJ. 2013. Maintenance of xylem network transport capacity: a review of embolism repair in vascular plants. *Frontiers in Plant Science* **4**: 108.

Brodersen CR, McElrone AJ, Choat B, Lee EF, Shackel KA, Matthews MA. 2013. *In vivo* visualizations of drought-induced embolism spread in Vitis vinifera. *Plant Physiology* **161**: 1820–1829.

Brodribb TJ, Cochard H. 2009. Hydraulic failure defines the recovery and point of death in water-stressed conifers. *Plant Physiology* **149**: 575–584.

Brodribb TJ, Hill RS. 1999. The importance of xylem constraints in the distribution of conifer species. *New Phytologist* **143**: 365–372.

Brodribb TJ, Holbrook NM. 2003. Stomatal closure during leaf dehydration, correlation with other leaf physiological traits. *Plant Physiology* **132**: 2166–2173.

Brodribb TJ, Holbrook NM. 2004. Diurnal depression of leaf hydraulic conductance in a tropical tree species. *Plant, Cell & Environment* **27**: 820–827.

Brodribb TJ, McAdam SA, Jordan GJ, Martins SC. 2014. Conifer species adapt to low-rainfall climates by following one of two divergent pathways. *Proceedings of the National Academy of Sciences, USA* **111**: 14489–14493.

Buckley TN. 2015. The contributions of apoplastic, symplastic and gas phase pathways for water transport outside the bundle sheath in leaves. *Plant, Cell & Environment* **38**: 7–22.

Choat B, Brodersen CR, McElrone AJ. 2015. Synchrotron X-ray microtomography of xylem embolism in *Sequoia sempervirens* saplings during cycles of drought and recovery. *New Phytologist* **205**: 1095–1105.

Choat B, Jansen S, Brodribb TJ, Cochard H, Delzon S, Bhaskar R, Bucci SJ, Feild TS, Gleason SM, Hacke UG *et al.* 2012. Global convergence in the vulnerability of forests to drought. *Nature* **7426**: 752–755.

Cochard H, Delzon S. 2013. Hydraulic failure and repair are not routine in trees. *Annals of Forest Science* **70**: 659–661.

Haines FM. 1935. Observations on the occurrence of air in conducting tracts. *Annals of Botany* **49**: 367–379.

Katifori E, Szöllősi GJ, Magnasco MO. 2010. Damage and fluctuations induce loops in optimal transport networks. *Physical Review Letters* **104**: 048704.

McCulloh KA, Meinzer FC. 2015. Further evidence that some plants can lose and regain hydraulic function daily. *Tree Physiology* **35**: 691–693.

Nardini A, Salleo S, Raimondo F. 2003. Changes in leaf hydraulic conductance correlate with leaf vein embolism in *Cercis siliquastrum* L. *Trees* **17**: 529–534.

Nolf M, Beikircher B, Rosner S, Nolf A, Mayr S. 2015. Xylem cavitation resistance can be estimated based on time-dependent rate of acoustic emissions. *New Phytologist* **208**: 625–632.

Ponomarenko A, Vincent O, Pietriga A, Cochard H, Badel É, Marmottant P. 2014. Ultrasonic emissions reveal individual cavitation bubbles in water-stressed wood. *Journal of The Royal Society Interface* **11**: 20140480.

Rockwell FE, Holbrook NM, Stroock AD. 2014a. The competition between liquid and vapor transport in transpiring leaves. *Plant Physiology* **164**: 1741–1758.

Rockwell FE, Wheeler JK, Holbrook NM. 2014b. Cavitation and its discontents: opportunities for resolving current controversies. *Plant Physiology* **164**: 1649–1660.

Sack L, Scoffoni C. 2013. Leaf venation: structure, function, development, evolution, ecology and applications in the past, present and future. *New Phytologist* **198**: 983–1000.

Salleo S, Lo Gullo MA, Raimondo F, Nardini A. 2001. Vulnerability to cavitation of leaf minor veins: any impact on leaf gas exchange? *Plant, Cell & Environment* **24**: 851–859.

Scoffoni C, Vuong C, Diep S, Cochard H, Sack L. 2014. Leaf shrinkage with dehydration: coordination with hydraulic vulnerability and drought tolerance. *Plant Physiology* **164**: 1772–1788.

Sperry JS, Pockman WT. 1993. Limitation of transpiration by hydraulic conductance and xylem cavitation in *Betula occidentalis*. *Plant, Cell & Environment* **16**: 279–287.

Triflio P, Nardini A, Lo Gullo MA, Salleo S. 2003. Vein cavitation and stomatal behaviour of sunflower (*Helianthus annuus*) leaves under water limitation. *Physiologia Plantarum* **119**: 409–417.

Tyree MT, Hammel HT. 1972. The measurement of the turgor pressure and the water relations of plants by the pressure-bomb technique. *Journal of Experimental Botany* **23**: 267–282.

Tyree MT, Sperry JS. 1989. Vulnerability of xylem to cavitation and embolism. *Annual Review of Plant Physiology and Plant Molecular Biology* **40**: 19–38.

Wheeler JK, Huggett BA, Tofte AN, Rockwell FE, Holbrook NM. 2013. Cutting xylem under tension or supersaturated with gas can generate PLC and the appearance of rapid recovery from embolism. *Plant, Cell & Environment* **36**: 1938–1949.

Supporting Information

Additional supporting information may be found in the online version of this article.

Fig. S1 Pressure–volume curves for the four species.

Please note: Wiley Blackwell are not responsible for the content or functionality of any supporting information supplied by the authors. Any queries (other than missing material) should be directed to the *New Phytologist* Central Office.